Arabian Journal of Chemistry (2020) 13, 9005–9018

King Saud University

Arabian Journal of Chemistry

www.ksu.edu.sa
www.sciencedirect.com

ORIGINAL ARTICLE

Facile synthesis of nanostructured Ni-Co/ZnO material: An efficient and inexpensive catalyst for Heck reactions under ligand-free conditions

Digambar B. Bankar [a,b], Kaluram G. Kanade [a,c,*], Ranjit R. Hawaldar [a], Sudhir S. Arbuj [a], Manish D. Shinde [a], Shrikant P. Takle [a], Dinesh P. Amalnerkar [d], Santosh T. Shinde [e]

[a] *Centre for Materials for Electronics Technology (C-MET), Panchwati, Off Pashan Road, Pune 411008, India*
[b] *P.G. Department of Chemistry, R. B. Narayanrao Borawake College, Shrirampur, Ahmednagar 413709, India*
[c] *P.G. and Research Centre, Yashavantrao Chavan Institute of Science, Satara 415001, India*
[d] *Department of Technology, Savitribai Phule Pune University (SPPU), Pune 411007, India*
[e] *P.G. Department of Chemistry, Maharaja Jivajirao Shinde Mahavidyalaya, Shrigonda, Ahmednagar 413701, India*

Received 23 July 2020; accepted 14 October 2020
Available online 29 October 2020

KEYWORDS

Nanostructured Ni-Co/ZnO material;
Heck reaction;
Phosphine ligand-free condition;
Heterogeneous catalyst

Abstract A simple, efficient and economically viable method for the Heck reaction has been accomplished in the absence of phosphine ligand. The Heck reaction was performed using nanostructured Ni-Co/ZnO material as a heterogeneous catalyst in a DMF/H_2O solvent system and in the presence of K_2CO_3, at 120 °C. The Ni-Co/ZnO nanostructures were prepared by the facile reduction-impregnation method. The structural and morphological properties of Ni-Co/ZnO nanostructure were investigated using various physico-chemical characterization techniques. Structural studies displayed the formation of hexagonal (wurtzite) ZnO. Electron microscopy imaging showed the presence of agglomerated clusters of Ni-Co nanoparticles over the surfaces of elliptical, flower bud-like and irregularly shaped sub-micron sized particle bundles of ZnO. The elemental composition analysis (EDX) confirmed the loading of Ni and Co nanoparticles over the nanocrystalline ZnO. The surface chemical state analysis of Ni-Co/ZnO material validated that Ni nanostructure exists in Ni^{2+} and Ni^{3+} species, whereas, Co nanostructure exists in Co^{2+} and Co^{3+} species. UV–Vis diffuse reflectance spectroscopy displays red shift in the light absorption edge of Ni-Co/ZnO catalyst compared to pure ZnO. The as-prepared Ni-Co bimetallic supported ZnO

* Corresponding author at: Centre for Materials for Electronics Technology (C-MET), Panchwati, Off Pashan Road, Pune 411008, India.
E-mail address: kgkanade@yahoo.co.in (K.G. Kanade).
Peer review under responsibility of King Saud University.

Production and hosting by Elsevier

https://doi.org/10.1016/j.arabjc.2020.10.023

nanostructure showed better catalytic activity and stability for the Heck reactions under phosphine ligand-free conditions. Ni-Co/ZnO catalyzed Heck reactions afforded the corresponding cross-coupled products with moderate to good yields (up to 92%). Ni-Co/ZnO catalyst could be reused for five successive runs without significant loss of catalytic activity.

1. Introduction

It is well known that the Heck reaction is one of the important cross-coupling reactions in synthetic organic transformations. The Heck reaction is also called Mizoroki-Heck reaction and is a powerful tool for the formation of carbon–carbon bonds between aryl halides and less substituted alkenes (olefins) and to generate the more substituted alkene compounds (Hosseini-Sarvari et al., 2014). The Mizoroki-Heck reaction was investigated simultaneously in the early 1970 s in the laboratories of Tsutomu Mizoroki and Richard Heck. The original reaction by Tsutomu Mizoroki in 1971 describes the coupling between iodobenzene and styrene using a $PdCl_2$ catalyst in methanol solvent to obtain stilbene (Mizoroki et al., 1971). In 1972, Richard F. Heck recognized the publication of Tsutomu Mizoroki and comprehended the work discovered independently. Richard F. Heck had reported the coupling between iodobenzene and styrene using $Pd(OAc)_2$ catalyst to form stilbene under solvent-free condition (Heck and Nolley, 1972). Richard Heck was awarded the Nobel Prize in Chemistry in 2010, jointly with Ei-ichi Negishi and Akira Suzuki for their significant work in the discovery and development of carbon–carbon bond forming reactions catalyzed by palladium (Johansson Seechurn et al., 2012).

The Heck reaction is one of the most extensively used palladium-catalyzed carbon–carbon coupling reactions and offers simplest way to synthesize variously substituted alkenes and many other unsaturated compounds which are used as dyes, UV screens and also useful as materials for optoelectronic devices (Beletskaya and Cheprakov, 2000). Heck reaction has been used in many fields such as natural product total synthesis (Dounay and Overman, 2003), fine chemicals (Blaser et al., 2004), pharmaceuticals and organic synthesis (Nadri et al., 2009). De Vries (2001) reported that the Heck reaction has been used in the manufacture of many important molecules, for example, Prosulfuron as an herbicide, octyl methoxycinnamate as a sunscreen agent, Naproxen as a nonsteroidal anti-inflammatory drug (NSAID) and Singulair as an antiasthma agent.

In the Mizoroki-Heck reaction, aryl iodides and bromides (Spencer, 1983), aryl chlorides (Spencer, 1984), aryl triflates (Ritter, 1993), aryl diazonium salts (Sengupta and Bhattacharya, 1993), aryl tosylates (Goegsig et al., 2009), arylsulfonyl hydrazides (Yuen et al., 2016), *etc*. reacted with alkenes in the presence of transition metal-based catalytic system and a suitable base, to produce carbon–carbon coupled products. The Mizoroki-Heck reaction can be performed by homogeneous as well as heterogeneous catalysis. Homogeneous catalysis has made a great impact on the development of Heck reactions. For instance, Moore and Shaughnessy (2004) have investigated the Heck reaction between aryl halides and alkenes using tri(4,6-dimethyl-3-sulfonatophenyl)phosphine trisodium and palladium acetate in CH_3CN:H_2O solvent system. The reactions were completed efficiently under mild reaction conditions with excellent yields. Homogeneous catalysis of Heck reaction is generally achieved by soluble palladium, mainly phosphine palladium complexes (Veisi and Mirzaee, 2018). However, phosphine ligands are expensive, non-recyclable, air-sensitive and toxic. In addition, the difficulty in recovery of palladium phosphine ligands not only increases production cost and adverse environmental impacts but also contaminates products, which limits their large scale application in the pharmaceutical and food industries (Bao et al., 2019).

To overcome or minimize the disadvantages of the homogeneous catalysis, significant efforts have been made to develop new methodologies for immobilizing homogeneous Pd catalysts on various solid supports. There are a number of reported methods in which palladium-based catalytic systems have been effectively used as heterogeneous catalysts in the Heck reactions. For instance, Ichikawa et al. (2018) have described the continuous-flow Mizoroki-Heck reaction catalyzed by Pd supported anion-exchange resin DIAION WA30 (i.e. Pd/WA30) under microwave irradiation and the reported catalyst could be reused up to five runs. The photochemical Heck reaction using a $PdCl_2/TiO_2$ catalyst under mild reaction conditions using DMF solvent and TEA (Et_3N) has been reported (Waghmode et al., 2013). Transition metal-based nanostructured materials play an important role in carbon–carbon bond forming reactions and effectively perform the Heck reactions under heterogeneous conditions. Yu et al. (2015) efficiently carried out the Heck reactions under ligand-free conditions using palladium nanoparticles supported on polyaniline (Pd@PANI) as a heterogeneous catalyst. Environment-friendly methods for the Heck reaction have been developed using Pd–Fe_3O_4 hybrid nanocrystals (Chung et al., 2013). Ye et al. (2019) have effectively embedded Pd nanoparticles into modified chitosan/PVA nanofibers by electrospinning technique and thermal treatment, and the resulting Pd-CS/PVA nanofiber mat used as an active and stable catalyst in the Heck reactions. The nanocrystalline Pd coated cordierite monolith material has been used as heterogeneous catalyst for the Heck reactions in DMF solvent under argon atmosphere (Bhat et al., 2019). Soni and Kotadia (2014) have investigated the time-dependent stereoselective Heck reaction performed by mesoporous Pd doped TiO_2 nanoparticles under sunlight. Literature survey also revealed that the Mizoroki-Heck reaction was carried out under ligand-free conditions using Pd supported ZnO nanoparticles (Hosseini-Sarvari et al., 2014).

The high cost of palladium systems has encouraged the researchers to search for less expensive transition metal catalysts as alternatives to the palladium systems for carbon–carbon cross-coupling reactions (Fürstner and Martin, 2005). Nickel, copper, iron and cobalt are among the most used transition metals other than palladium in the catalysis of cross-

coupling reactions (Hajipour et al., 2017). Cobalt and nickel catalysts are much cheaper, less toxic and readily available compared to palladium catalysts, consequently, a large number of catalytic transformations were achieved with Ni and Co catalysts in recent decade (Bao et al., 2019).

A review of the literature revealed that many researchers have developed cobalt-based effective catalyst systems, such as Co@MicroCS beads (Bao et al., 2019), flower-like cobalt nanostructures (Qi et al., 2009), carbon nanotube-encapsulated cobalt nanoparticles (Hajipour et al., 2019), Co hollow nanospheres (Zhou et al., 2007), Co/Al_2O_3 (Iyer and Thakur, 2000), Co-B amorphous alloy nanoparticles (Zhu et al., 2012), nano Co (Kumara et al., 2017), *etc.* and were applied in the Heck reactions. Recently, cobalt nanoparticles supported on modified magnetic chitosan with cyanuric chloride/melamine and also with 5-bromo-2-hydroxybenzalde hyde/cyanuric chloride have been used as heterogonous and efficient catalysts in the Heck reactions (Hajipour et al., 2020). Literature survey also disclosed that the nickel-based catalytic systems such as Ni/TPPTS immobilized on silica (Bhanage et al., 1998), Ni/Al_2O_3 (Iyer and Thakur, 2000), Ni nanoparticles (Zhang et al., 2009), carbon nanofibers/Ni(0) composite (Zhu et al., 2016), silica-supported poly-γ-aminopropylsilane Ni^{2+} complexes (Yang et al., 2003), *etc.* have been applied in carbon–carbon bond forming Heck reactions. Metal-organic frameworks (MOFs) and their derivatives find excellent applications in different fields viz. sensors, gas separation and storage, fine chemical synthesis, catalysis, electrochemical and biomedical applications (Konnerth et al., 2020), and in photovoltaic devices (Chueh et al., 2019). Liao et al. (2020) have investigated the use of MOF derived $AuPd@Co_3O_4$ (Au-Pd alloy nanoparticles-doped cobalt oxide) in the selective oxidation of 5-Hydroxymethylfurfural to 2,5- Furandicarboxylic acid. Besides, Liao et al. (2018) have reported the application of metal–organic framework-derived materials as effective solid catalysts for the valorization of Lignocellulosic biomass. Sulfonic acid functionalized mesoporous materials showed significant catalytic applications in large number of synthetic transformations (Doustkhah et al., 2019)

In recent decade, the development of nanostructured bimetallic catalysts has emerged as an important methodology to obtain a material with enhanced chemical and physical properties over their monometallic equivalents (Shan et al., 2014). The enhancement in the properties of nanostructured bimetallic catalysts is proved to be due to the substantial synergistic and cooperative interactions between individual metal components (structural and electron tuning) that modify the surface electronic properties (Rai et al., 2016a,b). In addition, the stability of the catalyst can be improved by the presence of a second counterpart in the air atmosphere, an aqueous condition and, therefore, improves the recyclability of the catalyst (Rai et al., 2016a,b). Heck reaction was also investigated with nanostructured bimetallic catalytic systems such as Au-Pd (Li et al., 2018a,b; Song et al., 2012) and Pd-Ni (Feng et al., 2015; Ohtaka et al., 2015).

In present work, we have performed the Heck reactions by replacing expensive Pd and Au noble metals with inexpensive and easily available non-noble transition metals like Ni and Co. Among the various metal oxide semiconductors, ZnO is a promising wide-band gap semiconductor and has been widely studied due to its excellent characteristics of low cost, good stability and non-toxicity (Kanade et al., 2007). Therefore, ZnO has been used in photocatalysis, heterogeneous catalysis and gas sensing applications. The use of suitable metal oxide support like ZnO improves the stability of bimetallic catalyst and can be used in the heterogeneous catalysis (Law et al., 2012).

In view of this, here, we report a simple and inexpensive method for the Heck cross-coupling reaction using nanostructured Ni-Co bimetallic supported ZnO material (Ni-Co/ZnO). Initially, nanocrystalline ZnO was prepared by a sol–gel method and further loading of Ni-Co bimetallic nanoparticles over ZnO nanoparticles was achieved by facile reduction-impregnation method. The as-synthesized nanocrystalline Ni-Co/ZnO material has been used as an inexpensive, non-toxic, recyclable and efficient catalyst for the Heck reactions under palladium and ligand-free conditions using a DMF/H_2O solvent system.

2. Experimental section

2.1. Materials

The reagents zinc acetate dihydrate [$Zn(OAc)_2{\cdot}2H_2O$], sodium hydroxide (NaOH), nickel chloride hexahydrate ($NiCl_2{\cdot}6H_2O$), cobalt chloride hexahydrate ($CoCl_2{\cdot}6H_2O$) and sodium borohydride ($NaBH_4$) required for the synthesis of nanocrystalline ZnO and Ni-Co/ZnO were obtained from S.D. Fine-Chem Limited and Loba Chemie Pvt. Ltd. All these reagents are of analytical grade and were used as received without further purification.

2.2. Synthesis of ZnO nanoparticles by sol–gel method

Initially, 0.5 M 250 mL solution of zinc acetate dihydrate, $Zn(OAc)_2{\cdot}2H_2O$ was taken in a 1000 mL beaker and stirred at room temperature for 10 min. To this solution, 1.0 M NaOH solution was slowly added drop-wise using dropping funnel with continuous magnetic stirring until the pH became 10. The resultant solution was further stirred at room temperature for 10 h. The residue was kept for 36 h at room temperature. Later, the formed gel (residue) was separated by filtration, washed with distilled water till the pH of the filtrate becomes neutral. Then the residue was dried at 120 °C for 10 h. Further, dried residue was calcined at 500 °C in a muffle furnace for 3 h. Then the obtained powder was allowed to cool, grinded in mortar with pestle and again calcined at 500 °C for 3 h in order to ensure complete decomposition of $Zn(OH)_2$ to ZnO.

2.3. Synthesis of nanostructured Ni-Co/ZnO material

The nanocrystalline Ni-Co/ZnO material was synthesized by facile reduction-impregnation method. In a typical procedure, $NiCl_2{\cdot}6H_2O$ (0.4 g) and $CoCl_2{\cdot}6H_2O$ (0.2 g) were dissolved in 30 mL distilled water. To it, $NaBH_4$ solution (0.3 g $NaBH_4$ in 30 mL EtOH) was added drop-wise with constant stirring. The resulting solution was stirred at room temperature for 1 h and then at 80 °C for 4 h. The solution is separated from the resulting black residue by filtration. Then residue in the round bottom flask was mixed with water (30 mL), stirred for 20 min and then allowed to settle down and water was separated. The same procedure was repeated using 20 mL ethanol. After-

wards, 30 mL ethanol was added to the obtained black residue followed by slow addition of 1.0 g of as-synthesized nanocrystalline ZnO powder under continuous magnetic stirring. The resulting mixture was stirred at room temperature for 1 h and then refluxed for 4 h. Finally, EtOH was evaporated under vacuum using a rotary evaporator. The obtained powder was dried in an oven at 120 °C for 4 h. Synthesis of nanocrystalline Ni/ZnO and Co/ZnO catalysts were accomplished by applying the same procedure for the sake of comparing the effect of only Ni and Co loading on ZnO nanoparticles on the Heck reaction. For the synthesis of Ni/ZnO, we used 0.4 g of $NiCl_2{\cdot}6H_2O$ and for the Co/ZnO synthesis; we used 0.4 g of $CoCl_2{\cdot}6H_2O$ A detailed scheme depicting the synthesis of a nanostructured Ni-Co/ZnO material and its further application in the Heck reaction is shown in Fig. 1.

2.4. Procedure for Heck reaction

In a typical Heck reaction, iodobenzene (1.0 mmol, 500 mg), styrene (1.5 mmol), K_2CO_3 (1.5 mmol), Ni-Co/ZnO catalyst (0.4 mmol, 195 mg) and DMF/H_2O (1:1, v/v, 10 mL) were added into a round bottom flask and stirred at 120 °C for 16 h under air atmosphere. The progress of the reaction was checked by thin layer chromatography (TLC). After completion of the reaction, the reaction mixture was cooled to the room temperature, diluted with ethyl acetate and the reaction mass was stirred at room temperature for 20 min to ensure the separation of product from the catalyst. Then the catalyst was separated and again washed with ethyl acetate. The combined centrifuges were mixed with water and the organic phase was separated by extraction, dried over anhydrous Na_2SO_4, filtered, and evaporated. The resultant crude product mass was purified by column chromatography to yield the desired product. The pure organic compounds were analyzed by ^{1}H NMR, ^{13}C NMR, and FTIR spectral techniques.

2.5. Characterization of nanostructured materials and organic compounds

Powder X-ray diffractometer (Rigaku MiniFlex-600) with Cu Kα (λ = 1.5406 Å) radiation was used to study the crystal structure and phase purity of the prepared nanomaterials. The surface morphology of nanostructured materials was observed with the field emission scanning electron microscope (FESEM, Hitachi S-4800). The elemental composition of Ni and Co in the catalyst was measured by energy-dispersive X-ray spectroscopy (EDX). The UV–Visible diffuse-reflectance spectra (DRS) were recorded using a UV–Vis diffuse-reflectance spectrophotometer (Perkin Elmer, Model Lambda 365). The X-ray photoelectron spectroscopic (XPS) scans were recorded by the Thermo Fisher Scientific instrument UK in order to establish the chemical states of elements in the nanocrystalline Ni-Co/ZnO material. All the XPS spectra were corrected using the adventitious C 1 s peak at 284.8 eV.

The progress of the Heck reactions was monitored by thin layer chromatography using Merck silica gel 60 F_{254} TLC plate. The purification of the desired organic products was accomplished by column chromatography technique using silica gel, 60–120 mesh, and n-hexane and ethyl acetate as an eluent. The ^{1}H NMR and ^{13}C NMR spectra of the Heck reaction products were acquired on a Bruker Ascend 500 NMR spectrometer operating at 500 MHz and 125 MHz, respectively, in $CDCl_3$ solvent. The ^{1}H and ^{13}C chemical shifts (δ) are reported in ppm relative to Tetramethylsilane (TMS), as the internal standard substance. The coupling constant (J) values are expressed in Hz. FT-IR spectra were acquired on Bruker spectrophotometer.

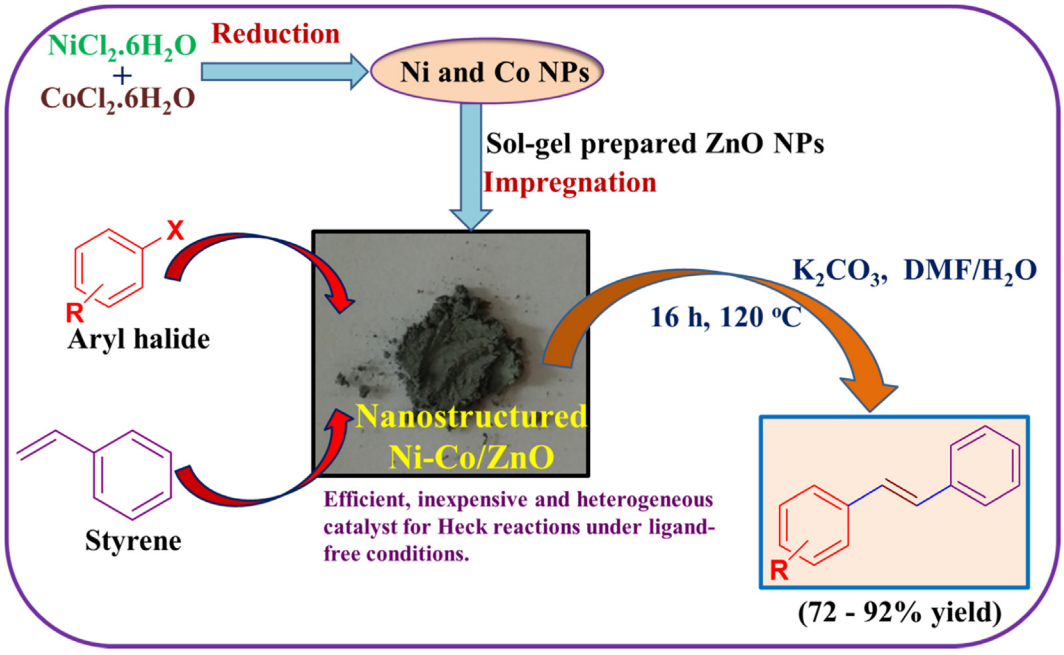

Fig. 1 A detailed scheme depicting the synthesis of nanostructured Ni-Co/ZnO material and its further application in the Heck reaction.

3. Results and discussion

3.1. X-ray diffraction (XRD)

XRD patterns of pure ZnO, Ni/ZnO, Co/ZnO, and Ni-Co/ZnO samples are displayed in Fig. 2. The prominent diffraction peaks associated with (100), (002), (101), (102), (110), (103), (112) and (201) planes were observed for all the synthesized samples. All the diffraction peaks are consistent with the hexagonal wurtzite structure which is identified for pristine ZnO (El-Hilo et al., 2019) and is in agreement with standard JCPDS card no. 36–1451, indicating the polycrystalline nature of all the samples (Fig. 2a–d). No additional crystalline phases of impurities were observed in the XRD patterns of all as-synthesized samples signifying the phase purity of all the samples. Besides, diffraction peaks for Ni and Co species were not detected, as expected. The absence of Ni and Co species demonstrates that Ni and Co ions are incorporated in ZnO lattice without altering the wurtzite structure of ZnO (Ali et al., 2018; Kocyigit and Topkaya, 2019; Vijayaprasath et al., 2016).

The crystallite size of all the as-synthesized samples was calculated by Scherrer's equation using the broadening of (101) peak of ZnO. The calculated crystallite sizes of powdered samples are shown in Table 1 and it should be noted that all the samples shows nearly the same crystallite size. It has been observed that 2θ values are marginally shifted to lower values for Ni, Co and Ni-Co loaded ZnO samples in comparison to unloaded ZnO indicating effective surface coating over ZnO and/or might be due to partial incorporation of Ni and Co in ZnO crystal lattice as shown in inset of Fig. 2 for (101) plane. The 2θ values of (101) plane for pure ZnO, Ni/ZnO, Co/ZnO and Ni-Co/ZnO nanocrystalline samples are around 36.28°, 36.22°, 36.24° and 36.18°, respectively. It should be noted that, the 2θ value of (101) plane for Ni-Co/ZnO sample was more shifted towards lower value compared to Ni/ZnO and Co/ZnO samples.

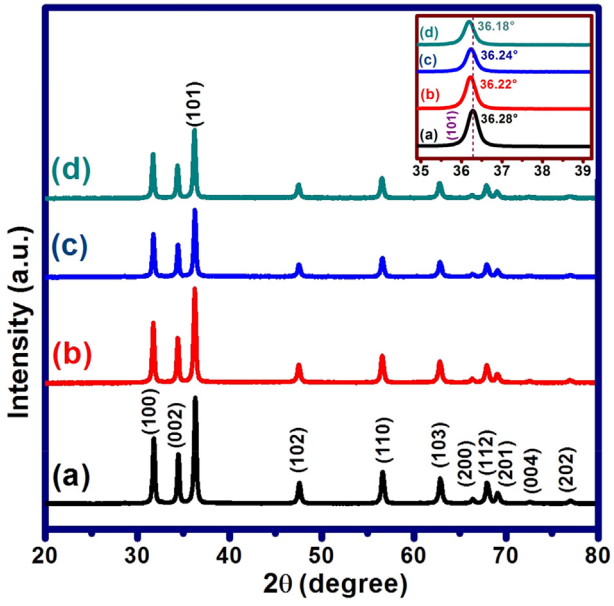

Fig. 2 XRD patterns of: (a) Pure ZnO, (b) Ni/ZnO, (c) Co/ZnO and (d) Ni-Co/ZnO powders. Inset is enlarged view of (101) plane.

Table 1 Calculated crystallite sizes of as-synthesized powdered samples.

Entry	Sample	Crystallite size (nm)
1	Pure ZnO	28
2	Ni/ZnO	29
3	Co/ZnO	27
4	Ni—Co/ZnO	27

3.2. Morphological and compositional characterization (FESEM and EDX analysis)

FESEM images of pure ZnO and Ni-Co loaded ZnO nanostructures are shown in Fig. 3. FESEM image corresponding to the pristine ZnO sample shows the formation of elliptical, flower bud-like and irregularly shaped sub-micron sized particle bundles (Fig. 3a). The length of the elliptic and bud-like morphologies varies in the range of 700 to 1500 nm while the thickness is in the range of 200 to 800 nm. The magnified image of a typical bud-like morphology in the inset of Fig. 3a reveals that such morphology is created by the agglomeration of beaded chain like nanostructures of size 30–50 nm. Elliptic and irregular shaped sub-micron sized morphologies also appear to be made up of such beaded chain like nanostructures.

FESEM image attributable to Ni-Co loaded ZnO sample as shown in Fig. 3b reveals the presence of agglomerated clusters of nanoparticles over the surfaces of elliptical, flower bud-like and irregularly shaped sub-micron sized particle bundles of ZnO. The magnified image of a typical ellipse like morphology of Ni-Co/ZnO in the inset of Fig. 3b reveals that such morphology is partially covered by the agglomerated nanoparticles of size 10–20 nm (which is speculated to be made up of Ni-Co, indicated by red colored circle and arrows). The distribution of these nanoparticles over ZnO nanostructure is random.

Fig. 4 represents the energy-dispersive X-ray (EDX) spectrum of Ni-Co/ZnO sample. The EDX spectrum reveals that Ni-Co/ZnO sample contains 75.80 wt% zinc, 15.59 wt% oxygen, 4.94 wt% of nickel and 3.67 wt% of cobalt and hence, clearly confirmed that Ni and Co elements were effectively supported over ZnO. The EDX spectrum also discloses that Ni-Co/ZnO contains 3.69 atomic % of Ni and 2.73 atomic % of Co. Inset of Fig. 4 shows the Table corresponding to elemental composition of the sample.

3.3. XPS analysis

X-ray photoelectron spectroscopy (XPS) is a material characterization technique typically used to determine the surface composition and chemical states according to the specific binding energies of various elements on the surface of materials. XPS analysis was performed in order to ascertain the chemical states of the Ni and Co elements in nanocrystalline Ni-Co/ZnO material. Fig. 5 represents the XPS survey spectrum and high resolution scans of different elements present in Ni-Co/ZnO material. Ni, Co, Zn and O elements are observed in the XPS survey spectrum of nanostructured Ni-Co/ZnO (Fig. 5a). In Fig. 5b, the binding energy peaks observed at 1021.3 eV and 1044.5 eV are allied with Zn $2p_{3/2}$ and Zn $2p_{1/2}$ energy states, respectively, signifying Zn^{2+} in ZnO (Mo

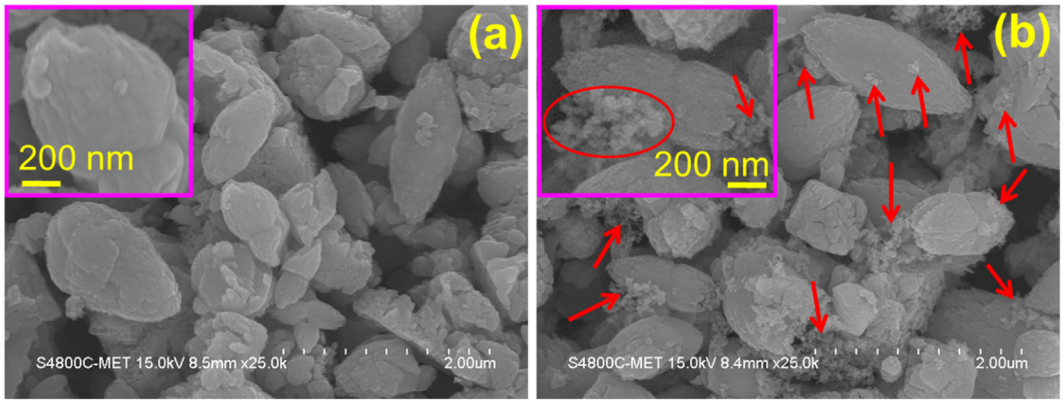

Fig. 3 FESEM images of (a) pristine ZnO and (b) Ni-Co/ZnO nanostructures.

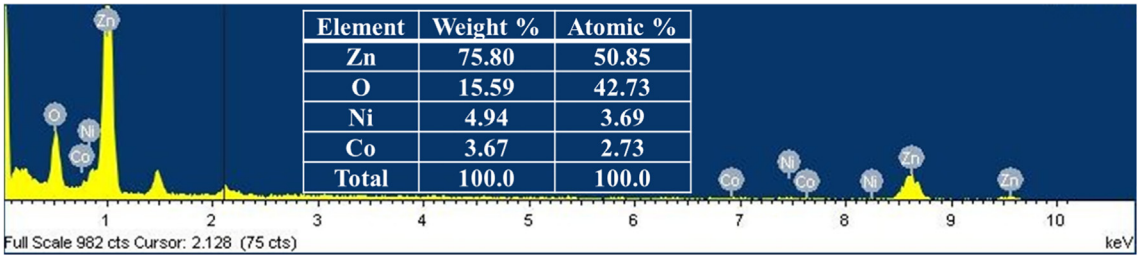

Element	Weight %	Atomic %
Zn	75.80	50.85
O	15.59	42.73
Ni	4.94	3.69
Co	3.67	2.73
Total	100.0	100.0

Fig. 4 FESEM-EDX spectrum of Ni-Co/ZnO catalyst.

et al., 2019). The XPS spectrum of O 1 s is depicted in Fig. 5c. The binding energy peak at 530.4 eV is attributed to lattice oxygen of ZnO (Hosseini-Sarvari et al., 2014). Fig. 5d represents the deconvoluted spectrum of Ni 2p core level in which Ni $2p_{3/2}$ and Ni $2p_{1/2}$ energy states are clearly observed at 855.0 eV and 873.1 eV, respectively. The energy difference between these two peaks is 18.1 eV indicating the Ni^{2+} state of Ni in NiO (Malevu et al., 2019). In addition, the Ni 2p deconvoluted spectrum shows the presence of Ni $2p_{3/2}$ peak at binding energy of 856.5 eV which validates the Ni^{3+} state of Ni in the form of Ni_2O_3 (Praveen and Jayakumar, 2019; Yu et al., 2001) and the Ni $2p_{1/2}$ peak at 875.0 eV has been also observed. Moreover, the weak binding energy peak of Ni 2p spectrum at 852.1 eV can be indorsed to the Ni^0 (Purohit et al., 2017). The other two peaks in the Ni 2p spectrum centered at 861.0 eV and 880.0 eV are attributed to Ni $2p_{3/2}$ and Ni $2p_{1/2}$ satellites, respectively.

The deconvolution spectrum of Co 2p core level is depicted in Fig. 5e in which the binding energy peaks of Co $2p_{3/2}$ and Co $2p_{1/2}$ are located at 780.2 eV and 795.8 eV, respectively, which can be fitted to Co^{3+} species (Li et al., 2018a,b; Wu et al., 2018). The observed energy difference between Co $2p_{3/2}$ and Co $2p_{1/2}$ is 15.6 eV. In addition, the peaks at 782.0 eV and 797.9 were corresponding to the Co $2p_{3/2}$ and Co $2p_{1/2}$ energy levels, respectively, which could be ascribed to Co^{2+} species (Li et al., 2018a,b). The Co 2p binding energy peaks observed at 780.2 eV and 795.8 eV are associated with Co_3O_4 (Chen et al., 2007; Liao et al., 2006). The other two peaks in the Co 2p scan centered at 785.7 eV and 802.1 eV are allied to the Co $2p_{3/2}$ and Co $2p_{1/2}$ satellites of Co species.

3.4. UV–Vis DRS analysis

Optical properties of pure ZnO, Ni/ZnO, Co/ZnO and Ni-Co/ZnO nanocrystalline samples were investigated using Ultraviolet–visible diffuse reflectance spectra (UV–Vis DRS). Fig. 6a displays the absorbance versus wavelength graph of unloaded and Ni, Co and Ni-Co loaded ZnO samples. The absorption spectra divulge that there is red shift of the light absorption edge of Ni/ZnO, Co/ZnO and Ni-Co/ZnO materials as compared to pure ZnO. The absorption edge of bare ZnO is at around 395 nm with corresponding band gap of 3.11 eV. By loading with Ni and Co elements, the absorption region gets altered, might be due to partial incorporation of Ni and Co elements in to the ZnO lattice. The metal Ni, Co and Ni-Co loaded ZnO samples exhibited a tailed absorption in the visible light (> 400 nm) region.

The optical band gap energy values of the as-synthesized nanostructures were investigated using the absorption band-edge according to Tauc's plot (Fig. 6b). The Tauc plot shows that there was a decrease in band gap energy for all metal loaded ZnO samples. The plot of $(\alpha h\nu)^2$ versus photon energy ($h\nu$) in eV between valence and conduction bands shows that pure ZnO displayed an energy threshold in the UV region corresponding to an estimated bulk energy band gap of 3.11 eV, while the band gap narrowing was observed for Ni, Co, and Ni-Co loaded ZnO materials. The calculated band gap values are 3.11, 3.01, 2.97 and 2.94 eV for unloaded ZnO, Ni/ZnO, Co/ZnO, Ni-Co/ZnO samples, respectively. The Tauc plot suggests that the incorporation of Ni, Co and Ni-Co in ZnO

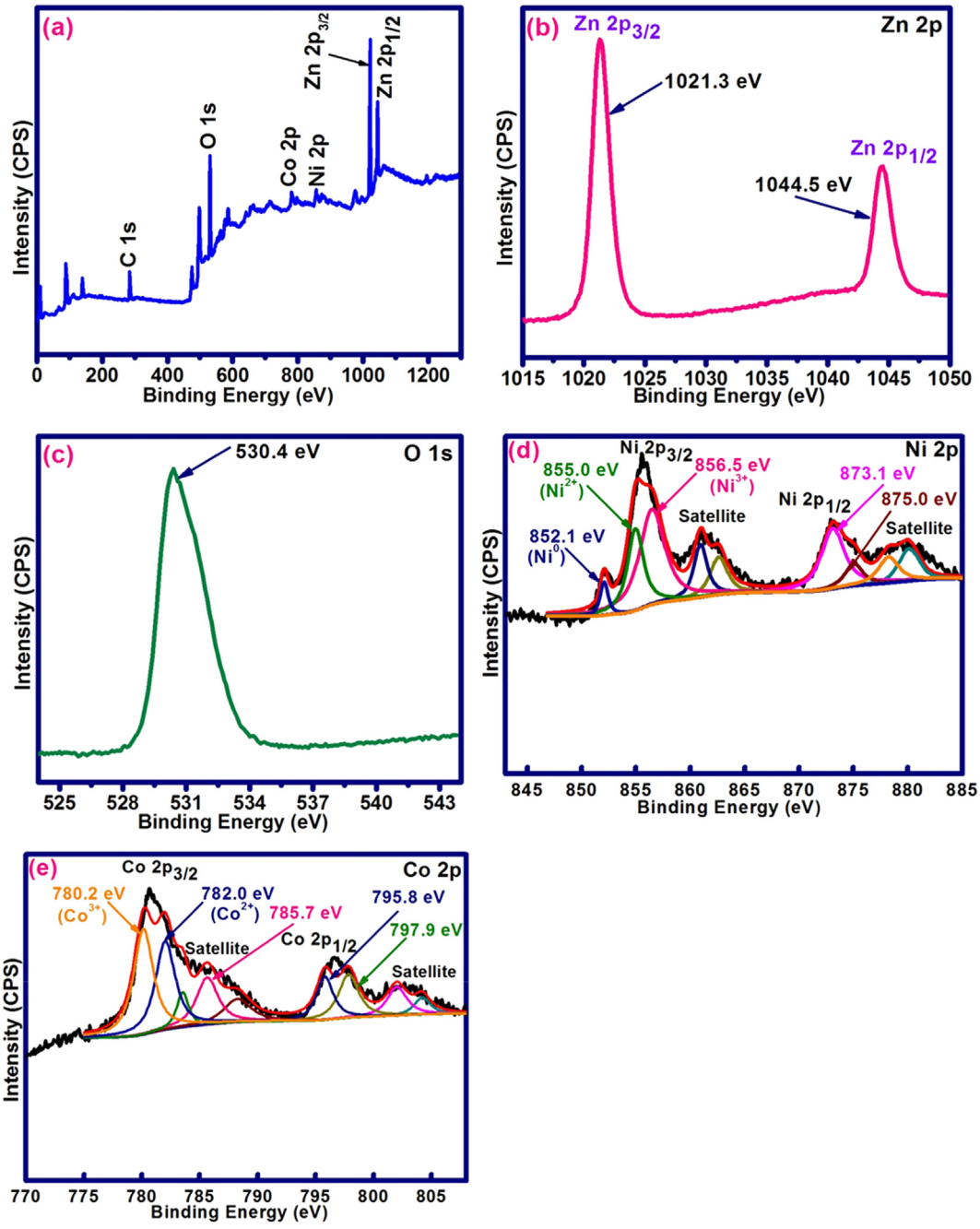

Fig. 5 (a) XPS survey spectrum of nanostructured Ni-Co/ZnO; (b) Zn 2p, (c) O 1 s, (d) Ni 2p and (e) Co 2p XPS spectra of Ni-Co/ZnO nanostructure.

shows marginal red shift in absorption edge to longer wavelength as well as increase in absorption in entire visible region. The red shift in band gap might be due to the sp-d exchange interactions between the band electrons of ZnO and the localized d-electrons of Ni and Co ions in metal loaded ZnO samples (Kocyigit and Topkaya, 2019).

3.5. FTIR analysis

The Fourier transform infrared (FTIR) spectra of pure ZnO, Ni/ZnO, Co/ZnO and Ni-Co/ZnO samples are measured in the range of 4000 to 400 cm^{-1} and are presented in Fig. 7. There is no extra peak observed in the range of 3300 to 3700 cm^{-1} (Fig. 7a) indicating the absence of monodentate O—H group which is from water (surface free or bonded). The absence of O—H peak at 3300 to 3700 cm^{-1} indicates that the complete formation of oxides. Spectral peaks at 1737 to 1218 cm^{-1} are related to C═O, C—C, C—O and C—H stretching vibrations (Hassanpour et al., 2019; Xiong et al., 2009). In FTIR spectra, the sharp peaks positioned at around 497 cm^{-1} and 567 cm^{-1} are attributed to the formation of Zn—O bond. Distinctive IR peaks less than 1000 cm^{-1} are very important to examine the presence of Zn—O, Ni—ZnO, Co—ZnO and

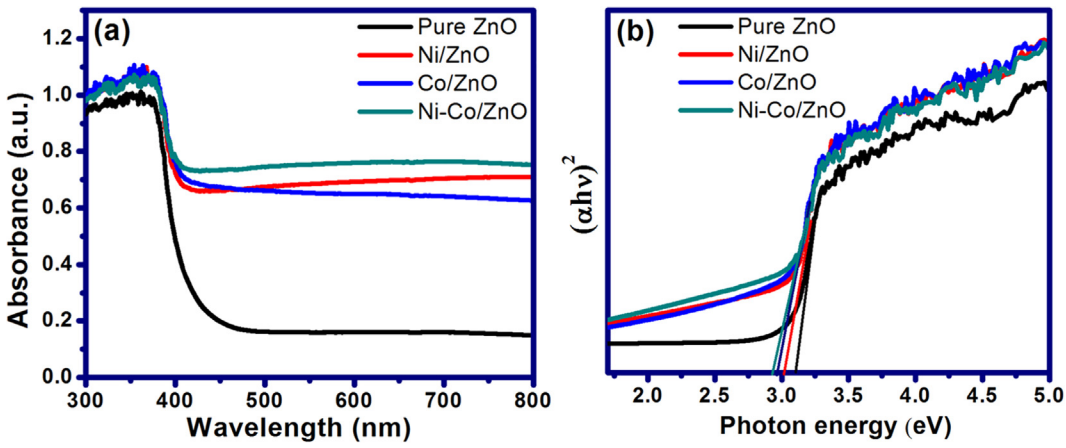

Fig. 6 (a) UV–Vis DRS spectrum and (b) Tauc's plot of unloaded ZnO and metal-loaded ZnO samples.

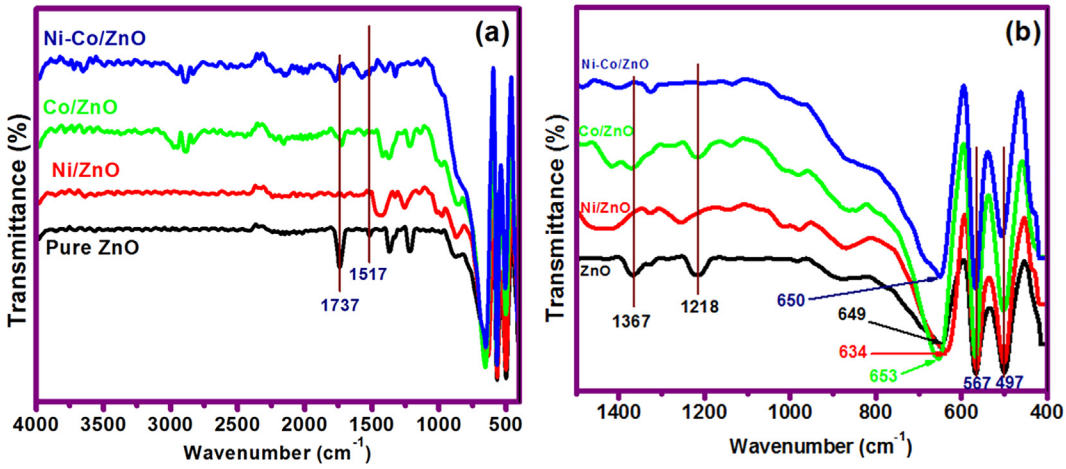

Fig. 7 FTIR spectra: (a) Pure ZnO and metal-loaded ZnO samples and (b) Enlarged view of the wavenumber (below 1500 cm^{-1}).

Ni—Co—Zn—O bonds. The FT-IR absorption bands observed around 649, 634, 653 and 650 cm^{-1} can be ascribed to the stretching modes of Zn—O, Ni—Zn—O, Co—Zn—O and Ni—Co—Zn—O nanostructured samples, respectively (Vijayaprasath et al., 2016), as shown in Fig. 7b.

3.6. Catalytic application of nanostructured Ni-Co/ZnO material

After a successful synthesis and characterization of nanocrystalline Ni/ZnO, Co/ZnO, and Ni—Co/ZnO materials, their catalytic performances were studied to accomplish the Heck reactions. The screening reactions were performed using iodobenzene and styrene as model substrates (Scheme 1).

For optimization of the reaction conditions, effects of the catalyst, solvent, base and temperature on the Heck coupling reaction of iodobenzene and styrene were studied and the summary of optimization is given in Table 2. The reaction did not occur with pure ZnO. When the reaction was carried out with Ni/ZnO in N, N-dimethylformamide (DMF) using NEt_3, the 64% yield was observed at 90 °C in 16 h (entry 2, Table 2). Using a DMF/H_2O (1:1, v/v) solvent and K_2CO_3 as a base for Ni/ZnO and Co/ZnO catalyzed Heck reactions, yields of 70% and 66% were obtained, respectively at 90 °C (entries 3–4, Table 2). However, when reaction was carried out at 120 °C for Ni/ZnO catalyst using DMF and NEt_3, a yield of 82% was obtained (entry 5, Table 2) and 74% yield for Co/ZnO (entry 6, Table 2). This means that with an increase in reaction temperature, an improvement in yield was observed.

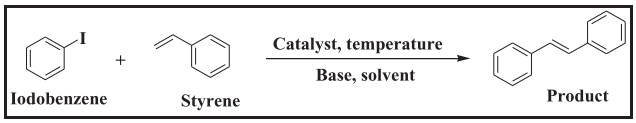

Scheme 1 Model Heck reaction.

Subsequently, we performed Heck reactions using nanocrystalline Ni and Co bimetallic supported ZnO material (Ni-Co/ZnO catalyst) and observed good results compared to monometallic Ni and Co supported ZnO catalysts. Ni-Co/ZnO provided a yield of 88% using DMF and NEt_3 (entry 7, Table 2), while using DMF/H_2O and K_2CO_3, a yield of 92% was obtained (entry 8, Table 2). For Na_2CO_3 as a base, a yield of 88% for the Heck reaction using Ni-Co/ZnO was obtained (entry 9, Table 2). The role of water as a co-solvent in the carbon–carbon cross coupling reactions is highly noticed

Table 2 Optimization of reaction conditions.[a]

Entry	Catalyst	Solvent	Base	Temp. (°C)	Yield[b] (%)
1	Pure ZnO	DMF	NEt_3	90	–
2	Ni/ZnO	DMF	NEt_3	90	64
3	Ni/ZnO	DMF/H_2O	K_2CO_3	90	70
4	Co/ZnO	DMF/H_2O	K_2CO_3	90	66
5	Ni/ZnO	DMF	NEt_3	120	82
6	Co/ZnO	DMF	NEt_3	120	74
7	Ni—Co/ZnO	DMF	NEt_3	120	88
8	Ni—Co/ZnO	DMF/H_2O	K_2CO_3	120	92
9	Ni—Co/ZnO	DMF/H_2O	Na_2CO_3	120	88
10	Ni—Co/ZnO	Toluene	NEt_3	110	58
11	Ni—Co/ZnO	CH_3CN	NEt_3	80	54
12	Ni—Co/ZnO	DMF	Morpholine	120	–

[a] Reaction conditions: Iodobenzene (1.0 mmol), styrene (1.5 mmol), Catalyst (0.4 mmol), Base (1.5 mmol), 16 h, Solvent, Temp.
[b] Isolated yield.

(Sherwood et al., 2019). The use of water as a polar co-solvent can induce the homogeneity of inorganic base (i.e. K_2CO_3) and reaction mixture which, in turn, can enhance the rate of reaction. The results indicated that good yield results have been obtained for inorganic bases in DMF/H_2O solvent system.

In addition, we have studied the Heck reaction using toluene and CH_3CN solvents; however, lower yields were observed (entries 10–11, Table 2). CH_3CN is less polar solvent than DMF, but due to its characteristic polarity, it could offer a conversion of 54% of desired product. It has been reported that the combination of amine base and less polar solvent such as toluene provide a convenient route for the formation of homogeneous solution in the Heck reaction (Sherwood et al., 2019). Therefore, here toluene could offer a yield of 58% using a nanostructured Ni-Co/ZnO catalyst in presence of triethylamine base (i.e. NEt_3). Furthermore, the boiling point of toluene is 110.6 °C; somewhat high to enhance the reaction rate. Heck reaction was also performed using morpholine as a base, but no product formation was observed (entry 12, Table 2). Morpholine is an unhindered secondary amine. The Heck reaction proceeds through the formation of π-allylic complexes which are susceptible to undergo nucleophilic attack with a secondary amine such as morpholine. This leads to the formation of tertiary allylic amine as a major product instead of desired alkene product (Heck, 2004). Therefore, morpholine could not give the desired alkene product.

Thus, we observed better results for the Heck reaction using nanostructured Ni-Co/ZnO material as compared to Ni/ZnO and Co/ZnO. The increase in catalytic activity for bimetallic Ni and Co supported ZnO nanomaterial can be attributed to important synergistic and cooperative interactions between individual metallic components (structural and electron tuning) which modify the surface electronic properties. Additionally, the stability of the catalyst can be enhanced by the presence of a second counterpart (Rai et al., 2016a,b). Kaur et al. (2018) reported that the two metal components of bimetallic nanoparticles shows improved bifunctional performance and also provide extra properties viz. strength, functionality, and stability to the nanostructured material.

The mmol concentration of Ni-Co/ZnO catalyst was also optimized to obtain the highest yield. For 0.1 mmol, a trace yield was observed (entry 1, Table 3). For 0.2 mmol of catalyst, the yield observed was 38% (entry 2, Table 3). A further increase in the mmol of Ni-Co/ZnO catalyst from 0.3 mmol to 0.4 mmol resulted in an increase in the product yield from 72% to 92% (entries 3–4, Table 3). By increasing the mmol of catalyst from 0.4 to 0.5, the almost similar yield was obtained (entry 5, Table 3). Therefore, 0.4 mmol of Ni-Co/ZnO catalyst was selected and further Heck reactions were performed using 0.4 mmol of nanostructured Ni-Co/ZnO.

Using the optimized reaction conditions, a variety of structurally different aryl halides were used in the Heck reaction using styrene (Scheme 2) to obtain the desired carbon–carbon coupled products (entries 1–10, Table 4). It is observed that aryl iodides (iodobenzene and 4-iodotoluene, entries 1 and 3, Table 4) can contribute more in the Heck reactions compared to aryl bromides (bromobenzene and 4-bromotoluene, entries 2 and 4, Table 4). The results showed that the aryl iodides containing electron-rich substituents get converted to the desired products with more yields (entries 5–6, Table 4) than aryl iodides with electron-withdrawing substituents (entries 7–8, Table 4). In addition, the Heck reaction using 3-iodopyridine was carried out; however, lower yield of 74% was observed (entry 9, Table 4). We have also investigated the role of Ni-Co/ZnO catalyst with respect to chlorobenzene (entry 10, Table 4), but observed negligible formation of the product. This might be due to the poor reactivity of chloro group in

Table 3 Optimization of mmol of Ni-Co/ZnO catalyst for Heck reaction between iodobenzene and styrene.[a]

Entry	mmol of Ni-Co/ZnO catalyst	Yield[b] (%)
1	0.1	Trace
2	0.2	38
3	0.3	72
4	0.4	92
5	0.5	92

[a] Reaction conditions: Iodobenzene (1.0 mmol), styrene (1.5 mmol), Ni-Co/ZnO, K_2CO_3 (1.5 mmol), 16 h, DMF/H_2O, 120 °C.
[b] Isolated yield.

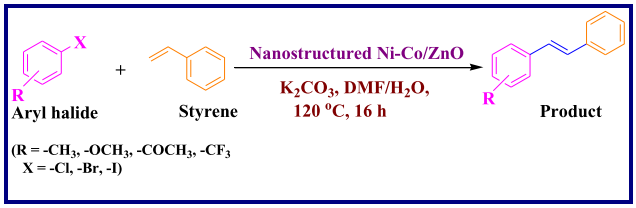

Scheme 2 General Heck reaction catalyzed by nanostructured Ni-Co/ZnO material.

such type of carbon–carbon bond forming reactions (Heck, 2004; Zhou et al., 2007).

Thus, Ni-Co/ZnO catalyzed Heck reaction generated the corresponding cross-coupled products with moderate to good yields (72% to 92%) at 120 °C using a polar DMF/H_2O solvent system and K_2CO_3 as a base in 16 h, under ligand-free conditions and in an air atmosphere.

In this work, we have performed Heck reaction under phosphine ligand-free conditions and in such reaction condition, there is absence of strongly bound neutral ligands. In order to facilitate the Heck reaction, phosphine-free catalytic systems can avail N, N-dimethylformamide (DMF) as a polar solvent with an aqueous medium (Beletskaya and Cheprakov, 2000). It has been also reported that the more polar DMF solvent promotes the oxidative addition and olefin insertion steps during the Heck reaction mechanism (Lin et al., 2004). The role of DMF has been noticed as a reducing agent as well as a solvent in many reactions (Carpenter et al., 2012; Jeong et al., 2009; Rai et al., 2016a,b), and broadly used for the reduction of metal ions (Bastakoti et al., 2015). Furthermore,

Table 4 Heck reaction of different aryl halides with styrene catalyzed by nanostructured Ni-Co/ZnO.[a]

Entry	Aryl halide	Styrene	Product	Yield[b] (%)
1			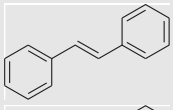	92
2			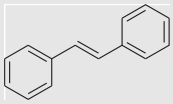	76
3	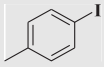		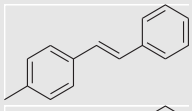	84
4	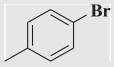		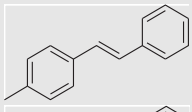	72
5	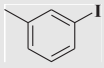		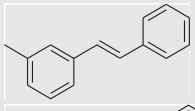	88
6	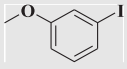		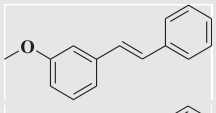	91
7	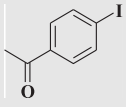		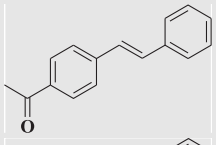	83
8	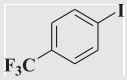		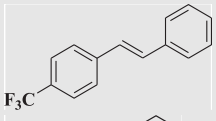	81
9		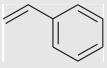	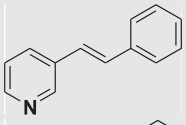	74
10		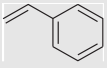	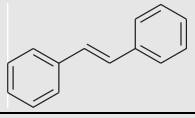	trace

[a] Reaction conditions: Aryl halide (1.0 mmol), styrene (1.5 mmol), Ni-Co/ZnO (0.4 mmol), K_2CO_3 (1.5 mmol), 16 h, DMF/H_2O (1:1, v/v), 120 °C, air atmosphere.

[b] Isolated yield.

DMF has sufficiently high boiling point (153 °C) to increase the rate of reaction (Sherwood et al., 2019). Therefore, in this work, we have performed Heck reactions using polar DMF solvent in combination with water (i.e. DMF/H_2O solvent system).

The plausible mechanism of the reaction between aryl halide and styrene over nanostructured Ni-Co/ZnO catalyst should be similar to the homogeneous Heck type mechanism (Scheme S1, ESI). In the first step (i.e. oxidative addition), nanostructured Ni-Co/ZnO catalyst (1) could inset in the aryl and halide bond to generate intermediate (2). In next step, intermediate (2) reacts with styrene and forms a π complex (3). In migratory insertion step, the styrene from the π complex (3) undergoes insertion with catalyst and aryl ring and produces intermediate (4). Next step is β hydride elimination step in which there is removal of hydrogen with the formation of π complex (5) on the surface of nanocatalyst. The π complex (5) then undergoes decomposition with removal of alkene product. The catalyst could regenerate in the final reductive elimination step by K_2CO_3 base. Here, we have assumed that the reduction of cationic Ni and Co nanoparticles supported by ZnO to active metallic Ni and Co could take place by the DMF solvent under the aqueous and basic reaction medium and this could complete the catalytic cycle of the Heck reaction.

Table 5 Recyclability of Ni-Co/ZnO catalyst in Heck reaction between iodobenzene and styrene.[a]

Run	Yield[b] (%)
1	92
2	90
3	84
4	81
5	76

[a] Reaction conditions: Iodobenzene (1.0 mmol), styrene (1.5 mmol), recycled catalyst, K_2CO_3 (1.5 mmol), 16 h, DMF/H_2O, 120 °C.
[b] Isolated yield.

The ^{1}H NMR, ^{13}C NMR and FT-IR spectral data of as-synthesized Heck reaction products are well matched to the desired products (see ESI). In addition, the observed coupling constant value (J = 16.5 Hz) for the olefin (alkene) protons clearly confirmed the formation of *trans*-substituted alkenes (Kaur et al., 2018) and not the cis isomer. In general, cis hydrogen atoms show the coupling constant value approximately of 10 Hz, while trans hydrogen atoms shows the coupling constant value of around 16 Hz (Pavia et al., 2008).

3.7. Recyclability study of the catalyst

The recyclability of catalyst is an essential factor from an economic and eco-friendly point of view. Consequently, the recyclability of Ni-Co/ZnO catalyst was checked in the Heck reaction between iodobenzene and styrene under the optimized reaction conditions. At the end of each reaction, the reaction mixture was allowed to cool to room temperature, the catalyst was separated, washed with ethyl acetate, dried at 100 °C for 4 h and reused. As shown in Table 5, the catalyst was reused five times without significant loss of catalytic activity and a yield of 76% was obtained after the fifth run for the heterogeneous catalyst.

3.8. Comparison of catalytic activities

We compared the catalytic activity of nanostructured Ni-Co/ZnO catalyst with some of the previously reported catalysts in the Heck reaction of iodobenzene and styrene, and the results are presented in Table 6. Obviously, some of the reaction conditions are mild and some reported methods shows better results. However, few of the reported methods required long reaction time, higher temperature and use of noble Pd or Au metals. The significant advantages of the present work are use of inexpensive and efficient Ni-Co/ZnO catalyst in the Heck reaction, heterogeneous catalysis, environmentally friendly method, minimization of metal contamination, and palladium and phosphine ligand-free conditions. Ni-Co/ZnO catalyzed Heck reaction offered the corresponding product with good yield. Moreover, the nanostructured Ni-Co/ZnO catalyst was synthesized by facile reduction-impregnation method.

Table 6 Comparison of catalytic activities of nanostructured Ni-Co/ZnO catalyst with literature examples for Heck reaction of iodobenzene with styrene.

Entry	Catalyst	Reaction conditions (Base, Solvent, Temperature)	Time (h)	Yield (%)	Ref.
1	Co/Al_2O_3	K_2CO_3, NMP, 150 °C	24	56	(Iyer and Thakur, 2000)
2	Nano Co	K_2CO_3, NMP, 140 °C	12	86	(Qi et al., 2009)
3	Co-B	K_2CO_3, DMF/H_2O, 120 °C	12	98	(Zhu et al., 2012)
4	Co@MicroCS	Et_3N, DMAc, 140 °C	8	65	(Bao et al., 2019)
5	Co-NHC@MWCNTs	Li_2CO_3, PEG, 80 °C	8	78	(Hajipour and Khorsandi, 2016)
6	"Si"~NH_2·$Co(OAc)_2$	Bu_3N, NMP, 150 °C	48	39	(Yang et al., 2003)
7	Ni-Pd	K_2CO_3, H_2O-DMF, 80 °C	9	48	(Rai et al., 2016a,b)
8	Ni nanoparticles	K_2CO_3, H_2O, 140 °C	16	78	(Zhang et al., 2009)
9	"Si"~NH_2·$Ni(OAc)_2$	Bu_3N, NMP, 150 °C	15	98	(Yang et al., 2003)
10	Pd/ZnO NPs	K_2CO_3, H_2O, 90 °C	17	95	(Hosseini-Sarvari et al., 2014)
11	Au-Pd	$NaHCO_3$, H_2O, 80 °C	3	80	(Song et al., 2012)
12	Ni/PANI composite	n-Pr_3N, DMF, 130 °C	36	69	(Houdayer et al., 2005)
13	Ni-Co/ZnO NPs	K_2CO_3, DMF/H_2O, 120 °C	16	92	Present work

4. Conclusions

In conclusion, we have easily prepared nanocrystalline Ni-Co/ZnO material by a simple reduction-impregnation method from the available starting materials. The synthesized Ni-Co/ZnO nanostructure was successfully used as a heterogeneous catalyst for the Heck reaction under ligand-free conditions without using an inert atmosphere. Ni-Co/ZnO material was used as a non-toxic and economically viable catalyst for the Heck reaction and retained reasonable catalytic activity for five successive runs. Ni-Co/ZnO nanomaterial included low-cost Ni and Co metallic systems compared to expensive noble metallic systems. We believe that this type of nanocrystalline bimetallic supported ZnO material finds excellent application as an active catalyst for other carbon–carbon bond formation reactions and a useful alternative to heterogeneous palladium catalysts. Furthermore, such type of nanocrystalline metal oxide system can acts as an active catalyst for laboratory-scale research and also for industrial applications.

Declaration of Competing Interest

The authors declare that they have no known competing financial interests or personal relationships that could have appeared to influence the work reported in this paper.

Acknowledgements

The author D.B. Bankar is grateful to the Director of C-MET Pune and the Principal of R. B. Narayanrao Borawake College, Shrirampur for providing necessary facilities. The administrative support of Rayat Shikshan Sanstha, Satara is sincerely acknowledged by Dr. K.G. Kanade. The authors express gratitude towards the Head of Chemistry department of Baburaoji Gholap College, Sangvi, Pune, and the Head and Project Assistants of Central Instrumentation Facility (CIF) department, Savitribai Phule Pune University, Pune for providing characterization facilities. This research did not receive any specific grant from funding agencies in the public, commercial, or not-for-profit sectors.

Appendix A. Supplementary material

Supplementary data to this article can be found online at https://doi.org/10.1016/j.arabjc.2020.10.023.

References

Ali, R.N., Naz, H., Li, J., Zhu, X., Liu, P., Xiang, B., 2018. Band gap engineering of transition metal (Ni/Co) codoped in zinc oxide (ZnO) nanoparticles. J. Alloys Compd. 744, 90–95.

Bao, Y., Shao, L., Xing, G., Qi, C., 2019. Cobalt, nickel and iron embedded chitosan microparticles as efficient and reusable catalysts for Heck cross-coupling reactions. Int. J. Biol. Macromol. 130, 203–212.

Bastakoti, B.P., Sakka, Y., Wu, K.C.W., Yamauchi, Y., 2015. Synthesis of highly photocatalytic TiO_2 microflowers based on solvothermal approach using N, N-dimethylformamide. J. Nanosci. Nanotechnol. 15, 4747–4751.

Beletskaya, I.P., Cheprakov, A.V., 2000. The Heck reaction as a sharpening stone of palladium catalysis. Chem. Rev. 100, 3009–3066.

Bhanage, B.M., Zhao, F., Shirai, M., Arai, M., 1998. Heck reaction using nickel/TPPTS catalyst and inorganic base on supported ethylene glycol phase. Catal. Lett. 54, 195–198.

Bhat, S.K., Prasad, J.D., Hegde, M.S., 2019. Recyclable Pd ionic catalyst coated on cordierite monolith for high TOF Heck coupling reaction. J. Chem. Sci. 131, 1–10.

Blaser, H.U., Indolese, A., Naud, F., Nettekoven, U., Schnyder, A., 2004. Industrial R & D on catalytic C-C and C-N coupling reactions: A personal account on goals, approaches and results. Adv. Synth. Catal. 346, 1583–1598.

Carpenter, M.K., Moylan, T.E., Kukreja, R.S., Atwan, M.H., Tessema, M.M., 2012. Solvothermal synthesis of platinum alloy nanoparticles for oxygen reduction electrocatalysis. J. Am. Chem. Soc. 134, 8535–8542.

Chen, Y., Zhang, Y., Fu, S., 2007. Synthesis and characterization of Co_3O_4 hollow spheres. Mater. Lett. 61, 701–705.

Chueh, C.C., Chen, C.I., Su, Y.A., Konnerth, H., Gu, Y.J., Kung, C. W., Wu, K.C.W., 2019. Harnessing MOF materials in photovoltaic devices: recent advances, challenges, and perspectives. J. Mater. Chem. A 7, 17079–17095.

Chung, J., Kim, J., Jang, Y., Byun, S., Hyeon, T., Kim, B.M., 2013. Heck and Sonogashira cross-coupling reactions using recyclable Pd–Fe_3O_4 heterodimeric nanocrystal catalysts. Tetrahedron Lett. 54, 5192–5196.

De Vries, J.G., 2001. The Heck reaction in the production of fine chemicals. Can. J. Chem. 79, 1086–1092.

Dounay, A.B., Overman, L.E., 2003. The asymmetric intramolecular Heck reaction in natural product total synthesis. Chem. Rev. 103, 2945–2964.

Doustkhah, E., Lin, J., Rostamnia, S., Len, C., Luque, R., Luo, X., Bando, Y., Wu, K.C.W., Kim, J., Yamauchi, Y., Ide, Y., 2019. Development of sulfonic-acid-functionalized mesoporous materials: Synthesis and catalytic applications. Chem. Eur. J. 25, 1614–1635.

El-Hilo, M., Dakhel, A.A., Yacoob, Z.J., 2019. Magnetic interactions in Co^{2+} doped ZnO synthesised by co-precipitation method: Efficient effect of hydrogenation on the long-range ferromagnetic order. J. Magn. Magn. Mater. 482, 125–134.

Feng, L., Chong, H., Li, P., Xiang, J., Fu, F., Yang, S., Yu, H., Sheng, H., Zhu, M., 2015. Pd–Ni alloy nanoparticles as effective catalysts for Miyaura-Heck coupling reactions. J. Phys. Chem. C 119, 11511–11515.

Fürstner, A., Martin, R., 2005. Advances in iron catalyzed cross coupling reactions. Chem. Lett. 34, 624–629.

Goegsig, T.M., Lindhardt, A.T., Dekhane, M., Grouleff, J., Skrydstrup, T., 2009. Heteroaromatic tosylates as electrophiles in regioselective Mizoroki–Heck-coupling reactions with electron-rich olefins. Chem. Eur. J. 15, 5950–5955.

Hajipour, A.R., Khorsandi, Z., 2016. Multi walled carbon nanotubes supported N-heterocyclic carbene–cobalt (II) as a novel, efficient and inexpensive catalyst for the Mizoroki-Heck reaction. Catal. Commun. 77, 1–4.

Hajipour, A.R., Rezaei, F., Khorsandi, Z., 2017. Pd/Cu-free Heck and Sonogashira cross-coupling reaction by Co nanoparticles immobilized on magnetic chitosan as reusable catalyst. Green Chem. 19, 1353–1361.

Hajipour, A.R., Khorsandi, Z., Farrokhpour, H., 2019. In situ synthesis of carbon nanotube-encapsulated cobalt nanoparticles by a novel and simple chemical treatment process: efficient and green catalysts for the Heck reaction. New J. Chem. 43, 8215–8219.

Hajipour, A.R., Khorsandi, Z., Abeshtiani, Z., Zakeri, S., 2020. Pd/Cu-free Heck and C-N coupling reactions using two modified magnetic chitosan cobalt catalysts: efficient, inexpensive and green heterogeneous catalysts. J. Inorg. Organomet. Polym. Mater. 30, 2163–2171.

Hassanpour, M., Salavati-Niasari, M., Tafreshi, S.A.H., Safardoust-Hojaghan, H., Hassanpour, F., 2019. Synthesis, characterization and antibacterial activities of Ni/ZnO nanocomposites using bis

(salicylaldehyde) complex precursor. J. Alloys Compd. 788, 383–390.
Heck, R.F., Nolley Jr, J.P., 1972. Palladium-catalyzed vinylic hydrogen substitution reactions with aryl, benzyl, and styryl halides. J. Org. Chem. 37, 2320–2322.
Heck, R.F., 2004. Palladium-catalyzed vinylation of organic halides. Org. React. 27, 345–390.
Hosseini-Sarvari, M., Razmi, Z., Doroodmand, M.M., 2014. Palladium supported on zinc oxide nanoparticles: Synthesis, characterization, and application as heterogeneous catalyst for Mizoroki-Heck and Sonogashira reactions under ligand-free and air atmosphere conditions. Appl. Catal. A. 475, 477–486.
Houdayer, A., Schneider, R., Billaud, D., Ghanbaja, J., Lambert, J., 2005. New polyaniline/Ni (0) nanocomposites: synthesis, characterization and evaluation of their catalytic activity in Heck couplings. Synth. Met. 151, 165–174.
Ichikawa, T., Mizuno, M., Ueda, S., Ohneda, N., Odajima, H., Sawama, Y., Monguchi, Y., Sajiki, H., 2018. A practical method for heterogeneously-catalyzed Mizoroki-Heck reaction: Flow system with adjustment of microwave resonance as an energy source. Tetrahedron 74, 1810–1816.
Iyer, S., Thakur, V.V., 2000. The novel use of Ni Co, Cu and Mn heterogeneous catalysts for the Heck reaction. J. Mol. Catal. A: Chem. 157, 275–278.
Jeong, G.H., Kim, M., Lee, Y.W., Choi, W., Oh, W.T., Park, Q.H., Han, S.W., 2009. Polyhedral Au nanocrystals exclusively bound by 110 facets: the rhombic dodecahedron. J. Am. Chem. Soc. 131, 1672–1673.
Johansson Seechurn, C.C., Kitching, M.O., Colacot, T.J., Snieckus, V., 2012. Palladium-catalyzed cross-coupling: a historical contextual perspective to the 2010 Nobel Prize. Angew. Chem. Int. Ed. 51, 5062–5085.
Kanade, K.G., Kale, B.B., Baeg, J.O., Lee, S.M., Lee, C.W., Moon, S. J., Chang, H., 2007. Self-assembled aligned Cu doped ZnO nanoparticles for photocatalytic hydrogen production under visible light irradiation. Mater. Chem. Phys. 102, 98–104.
Kaur, N., Kaur, G., Bhalla, A., Dhau, J.S., Chaudhary, G.R., 2018. Metallosurfactant based Pd–Ni alloy nanoparticles as a proficient catalyst in the Mizoroki Heck coupling reaction. Green Chem. 20, 1506–1514.
Kocyigit, A., Topkaya, R., 2019. Structural, optical and magnetic properties of Ni-Co co-doped ZnO thin films. Mater. Res. Express. 6, 096116.
Konnerth, H., Matsagar, B.M., Chen, S.S., Prechtl, M.H., Shieh, F.K., Wu, K.C.W., 2020. Metal-organic framework (MOF)-derived catalysts for fine chemical production. Coord. Chem. Rev. 416, 213319.
Kumara, K.J., Krishnamurthy, G., Swamy, B.K., Kumar, N.S., Kumar, M., 2017. Catalytic performance study of nano-cobalt: a catalyst for complement to the Heck coupling reaction. J. Porous Mater. 24, 1095–1103.
Law, Y.T., Skala, T., Pis, I., Nehasil, V., Vondracek, M., Zafeiratos, S., 2012. Bimetallic nickel–cobalt nanosized layers supported on polar ZnO surfaces: Metal–support interaction and alloy effects studied by synchrotron radiation X-ray photoelectron spectroscopy. J. Phys. Chem. C 116, 10048–10056.
Li, J., Wang, Y., Jiang, S., Zhang, H., 2018a. Facile synthesis of magnetic recyclable palladium-gold alloy nanoclusters catalysts $PdAu_r/Fe_3O_4$@LDH and its catalytic applications in Heck reaction. J. Organomet. Chem. 878, 84–95.
Li, Y., Li, F.M., Meng, X.Y., Wu, X.R., Li, S.N., Chen, Y., 2018b. Direct chemical synthesis of ultrathin holey iron doped cobalt oxide nanosheets on nickel foam for oxygen evolution reaction. Nano Energy 54, 238–250.
Liao, C.L., Lee, Y.H., Chang, S.T., Fung, K.Z., 2006. Structural characterization and electrochemical properties of RF-sputtered nanocrystalline Co_3O_4 thin-film anode. J. Power Sources 158, 1379–1385.
Liao, Y.T., Matsagar, B.M., Wu, K.C.W., 2018. Metal–organic framework (MOF)-derived effective solid catalysts for valorization of lignocellulosic biomass. ACS Sustain. Chem. Eng. 6, 13628–13643.
Liao, Y.T., Van Chi, N., Ishiguro, N., Young, A.P., Tsung, C.K., Wu, K.C.W., 2020. Engineering a homogeneous alloy-oxide interface derived from metal-organic frameworks for selective oxidation of 5-hydroxymethylfurfural to 2, 5-furandicarboxylic acid. Appl. Catal. B 270, 118805.
Lin, B.L., Liu, L., Fu, Y., Luo, S.W., Chen, Q., Guo, Q.X., 2004. Comparing nickel-and palladium-catalyzed Heck reactions. Organometallics 23, 2114–2123.
Malevu, T.D., Mwankemwa, B.S., Ahmed, M.A., Motaung, T.E., Tshabalala, K.G., Ocaya, R.O., 2019. Effect of Ni doping on ZnO nanorods synthesized using a low-temperature chemical bath. J. Electron. Mater. 48, 6954–6963.
Mizoroki, T., Mori, K., Ozaki, A., 1971. Arylation of olefin with aryl iodide catalyzed by palladium. Bull. Chem. Soc. Jpn. 44. 581–581.
Mo, Y., Shi, F., Qin, S., Tang, P., Feng, Y., Zhao, Y., Li, D., 2019. Facile fabrication of mesoporous hierarchical Co-doped ZnO for highly sensitive ethanol detection. Ind. Eng. Chem. Res. 58, 8061–8071.
Moore, L.R., Shaughnessy, K.H., 2004. Efficient aqueous-phase Heck and Suzuki couplings of aryl bromides using tri(4,6-dimethyl-3-sulfonatophenyl)phosphine trisodium salt (TXPTS). Org. Lett. 6, 225–228.
Nadri, S., Joshaghani, M., Rafiee, E., 2009. Biphenyl-based phosphine: A well-defined, air-stable, and efficient ligand for the Mizoroki-Heck reaction. Appl. Catal. A 362, 163–168.
Ohtaka, A., Sansano, J.M., Nájera, C., Miguel-García, I., Berenguer-Murcia, Á., Cazorla-Amorós, D., 2015. Palladium and bimetallic palladium–nickel nanoparticles supported on multiwalled carbon nanotubes: Application to carbon-carbon bond-forming reactions in water. ChemCatChem 7, 1841–1847.
Pavia, D.L., Lampman, G.M., Kriz, G.S., Vyvyan, J.A., 2008. Introduction to spectroscopy. Cengage Learning.
Praveen, E., Jayakumar, K., 2019. Investigations on structural, optical and ferromagnetic properties of Ni doped ZnO nanotwins. Mater. Sci. Semicond. Process. 102, 104609.
Purohit, P., Seth, K., Kumar, A., Chakraborti, A.K., 2017. C-O bond activation by nickel–palladium hetero-bimetallic nanoparticles for Suzuki-Miyaura reaction of bioactive heterocycle-tethered sterically hindered aryl carbonates. ACS Catal. 7, 2452–2457.
Qi, H., Zhang, W., Wang, X., Li, H., Chen, J., Peng, K., Shao, M., 2009. Heck reaction catalyzed by flower-like cobalt nanostructures. Catal. Commun. 10, 1178–1183.
Rai, R.K., Gupta, K., Tyagi, D., Mahata, A., Behrens, S., Yang, X., Xu, Q., Pathak, B., Singh, S.K., 2016a. Access to highly active Ni–Pd bimetallic nanoparticle catalysts for C-C coupling reactions. Catal. Sci. Technol. 6, 5567–5579.
Rai, R.K., Tyagi, D., Gupta, K., Singh, S.K., 2016b. Activated nanostructured bimetallic catalysts for C-C coupling reactions: recent progress. Catal. Sci. Technol. 6, 3341–3361.
Ritter, K., 1993. Synthetic transformations of vinyl and aryl triflates. Synthesis 1993 (08), 735–762.
Sengupta, S., Bhattacharya, S., 1993. Heck reaction of arenediazonium salts: a palladium-catalysed reaction in an aqueous medium. J. Chem. Soc. Perkin Trans. 1 (17), 1943–1944.
Shan, S., Luo, J., Yang, L., Zhong, C.J., 2014. Nanoalloy catalysts: structural and catalytic properties. Catal. Sci. Technol. 4, 3570–3588.
Sherwood, J., Clark, J.H., Fairlamb, I.J., Slattery, J.M., 2019. Solvent effects in palladium catalysed cross-coupling reactions. Green Chem. 21, 2164–2213.
Song, H.M., Moosa, B.A., Khashab, N.M., 2012. Water-dispersable hybrid Au–Pd nanoparticles as catalysts in ethanol oxidation, aqueous phase Suzuki-Miyaura and Heck reactions. J. Mater. Chem. 22, 15953–15959.

Soni, S.S., Kotadia, D.A., 2014. Time-dependent stereoselective Heck reaction using mesoporous Pd/TiO_2 nanoparticles catalyst under sunlight. Catal. Sci. Technol. 4, 510–515.

Spencer, A., 1983. A highly efficient version of the palladium-catalysed arylation of alkenes with aryl bromides. J. Organomet. Chem. 258, 101–108.

Spencer, A., 1984. Homogeneous palladium-catalysed arylation of activated alkenes with aryl chlorides. J. Organomet. Chem. 270, 115–120.

Veisi, H., Mirzaee, N., 2018. Ligand-free Mizoroki–heck reaction using reusable modified graphene oxide-supported Pd(0) nanoparticles. Appl. Organometal. Chem. 32, e4067.

Vijayaprasath, G., Murugan, R., Asaithambi, S., Babu, G.A., Sakthivel, P., Mahalingam, T., Hayakawa, Y., Ravi, G., 2016. Structural characterization and magnetic properties of Co co-doped Ni/ZnO nanoparticles. Appl. Phys. A 122, 122.

Waghmode, S.B., Arbuj, S.S., Wani, B.N., 2013. Heterogeneous photocatalysed Heck reaction over $PdCl_2/TiO_2$. New J. Chem. 37, 2911–2916.

Wu, P.R., Wu, C.L., Chen, D.H., 2018. Synthesis and controlled sulfidation of Ni-Co alloy on reduced graphene oxide as an electrode with enhanced conductivity and capacitance for supercapacitors. J. Alloys Compd. 735, 409–416.

Xiong, H.M., Shchukin, D.G., Möhwald, H., Xu, Y., Xia, Y.Y., 2009. Sonochemical synthesis of highly luminescent zinc oxide nanoparticles doped with magnesium (II). Angew. Chem. 121, 2765–2769.

Yang, Y., Zhou, R., Zhao, S., Li, Q., Zheng, X., 2003. Silica-supported poly-γ-aminopropylsilane Ni^{2+}, Cu^{2+}, Co^{2+} complexes: efficient catalysts for Heck vinylation reaction. J. Mol. Catal. A: Chem. 192, 303–306.

Ye, Z., Zhang, B., Shao, L., Xing, G., Qi, C., Tao, H., 2019. Palladium nanoparticles embedded chitosan/poly (vinyl alcohol) composite nanofibers as an efficient and stable heterogeneous catalyst for Heck reaction. J. Appl. Polym. Sci. 136, 48026.

Yu, G.H., Zeng, L.R., Zhu, F.W., Chai, C.L., Lai, W.Y., 2001. Magnetic properties and X-ray photoelectron spectroscopy study of NiO/NiFe films prepared by magnetron sputtering. J. Appl. Phys. 90, 4039–4043.

Yu, L., Huang, Y., Wei, Z., Ding, Y., Su, C., Xu, Q., 2015. Heck reactions catalyzed by ultrasmall and uniform Pd nanoparticles supported on polyaniline. J. Org. Chem. 80, 8677–8683.

Yuen, O.Y., So, C.M., Kwong, F.Y., 2016. Open-air oxidative Mizoroki-Heck reaction of arylsulfonyl hydrazides with alkenes. RSC Adv. 6, 27584–27589.

Zhang, W., Qi, H., Li, L., Wang, X., Chen, J., Peng, K., Wang, Z., 2009. Hydrothermal Heck reaction catalyzed by Ni nanoparticles. Green Chem. 11, 1194–1200.

Zhou, P., Li, Y., Sun, P., Zhou, J., Bao, J., 2007. A novel Heck reaction catalyzed by Co hollow nanospheres in ligand-free condition. Chem. Commun. 14, 1418–1420.

Zhu, Y., Bai, J., Wang, J., Li, C., 2016. Novel carbon nanofiber-supported Ni(0) nanoparticles catalysed the Heck reaction under ligand-free conditions. RSC Adv. 6, 29437–29440.

Zhu, Z., Ma, J., Xu, L., Xu, L., Li, H., Li, H., 2012. Facile synthesis of Co–B amorphous alloy in uniform spherical nanoparticles with enhanced catalytic properties. ACS Catal. 2, 2119–2125.